Optical Investigation of a regularized shear layer for the examination of the aero-optical component of the jitter

Matthew R. Kemnetz[1], Eric J. Jumper[2], and Stanislav Gordeyev[3]
University of Notre Dame, Notre Dame, IN, 46556

I. Introduction

Airborne laser systems are a significant interest to the aerospace community. They have many applications including high-bandwidth communication, strategic missile defense, and aircraft point defense. Airborne laser systems also carry with them unique challenges. One of those challenges is the aero-optics problem.

The aero-optics problem arises when an optical wavefront encounters a usually turbulent, time-varying flow field. The wavefront is aberrated by the changing index of refraction of the flow field caused by changes in fluid density. When a laser is shone through the flow field described, the beam becomes highly distorted. The aero-optics problem, which limits the lethal field of regard, has proved to be quite a challenge for airborne laser systems.

Traditionally gimbaled turrets have been used as convenient laser pointing devices in airborne platforms. Gimbaled turrets provide a large field of regard. This large field of regard is typically very important for communication, and point defense applications. A simplified diagram of the compressible flow topology over a canonical turret can be seen in Fig. [1].

---

[1] Ph.D. Candidate, University of Notre Dame, AIAA Student Member.
[2] Roth-Gibson Professor,University of Notre Dame
[3] Associate Professor, University of Notre Dame, AIAA Associate Fellow.

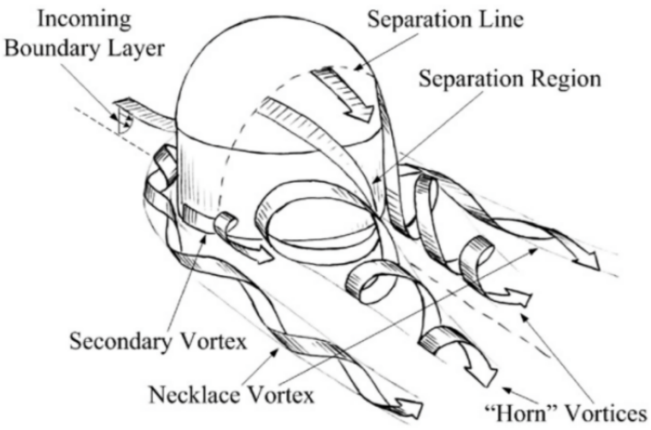

Fig. 1 Typical flow topology over a canonical turret.[1]

On the surface of the turret a turbulent boundary layer grows until a point is reached at which the flow separates. Behind the turret a separated wake region forms and large "horn" vortices develop. Around the base of the turret "necklace" vortices form. Past the separation line there is a significant shear layer. Finally in the transonic or supersonic flow regime shocks form on the turret. All of the described flow features carry with them significant density fluctuations.

These density fluctuations manifest as index of refraction fluctuations as per the Gladstone-Dale relation.[2],

$$n(x, y, z, t) = 1 + K_{GD}(\lambda)\rho(x, y, z, t) \tag{1}$$

In Eq. [1] $K_{GD}(\lambda)$ is the Gladstone-Dale constant for a given wavelength, λ. As a planar incident wavefront propagates through this spatio-temporally varying index of refraction field the phase velocity of the light will be perturbed. This causes constructive and destructive interference and an overall distorted beam.

In this work we focus on examining shear layers as they relate to aero-optic flows. Shear layers are a very significant contributor to overall aero-optic distortions in conventional systems.[3] Shear layers, due to their periodic vortical structures, contribute significantly to the aero-optical component of the jitter. In this work we leverage the previously developed stitching method[4] to study the aero-optical component of the jitter due to a shear layer. In this work, we focus on forced shear layers as forcing regularizes the shear layer over the aperture. But, the computational

machinery and methods are developed to be applied to natural shear layers in future work.

II. Experimental Measurements

The experiment was conducted in Notre Dame's Tr-Sonic Facility. The facility is an in-draft tunnel and the test section used is comprised of two inlets. The high speed inlet was set to $M = 0.6$. The center of the aperture was set at $27.5cm$ downstream of the splitter plate.

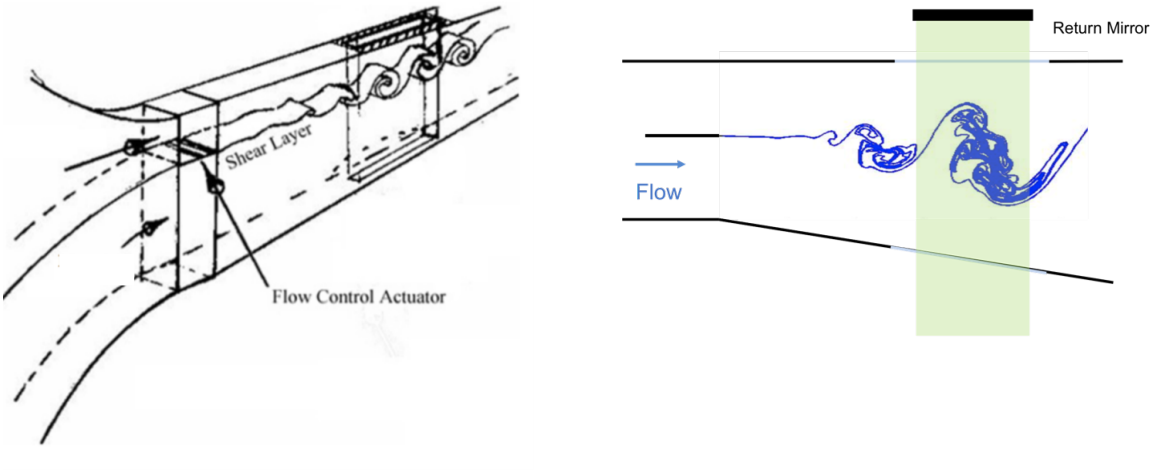

(a) Isometric view of the shear layer facility.

(b) Spanwise view of the shear layer facility.

Fig. 2 I will make better diagrams using my CAD diagram. Schematic of Notre Dame's Tri-Sonic Facility with the shear layer test section installed.

Voice coil actuators were mounted on the splitter plate to periodically force the shear layer. For more information on how the forcing was conducted see [5, 6]. The forcing frequency for this experiment was chosen to be 700 Hz. This has been shown to be a good choice of forcing frequency to regularize the shear layer for the streamwise location of our measurements.[5] The sampling frequency was set at 56kHz and full 2D wavefronts were collected. The wavefronts collected had 14 subapertures in the spanwise direction and 49 subapertures in the streamwise direction.

III. Results

To demonstrate the effect of forcing the shear layer, both forced and unforced data was collected. This allowed us to compare results between the two cases and show that shear layer forcing prevents shear layer growth over the aperture.

In this work we utilize the stitching method of wavefront reconstruction which is described in detail in [4]. The stitching method leverages the largely convective nature of the aero-optical structures to trade time for space and stitch neighboring frames of wavefront data together. In this manner, tip, tilt, and piston are reintroduced in the overlapping region between frames. A schematic of the stitching process can be seen in Figure [3]

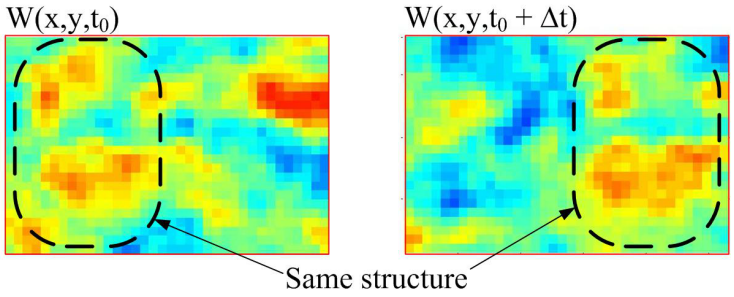

(a) The two frames to be stitched have common structures

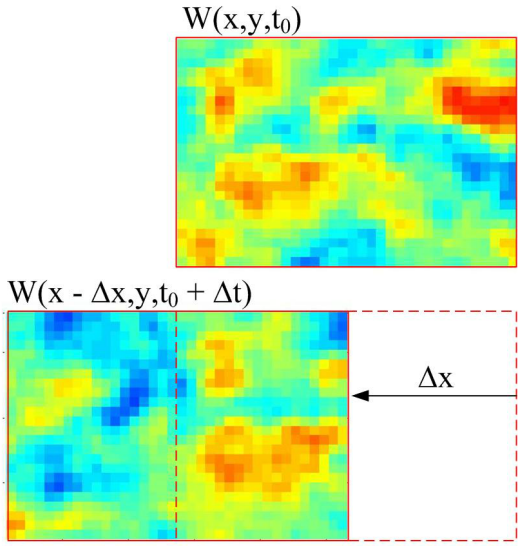

(b) The frame represented as $W(x, y, t+\Delta t)$ is shifted in space

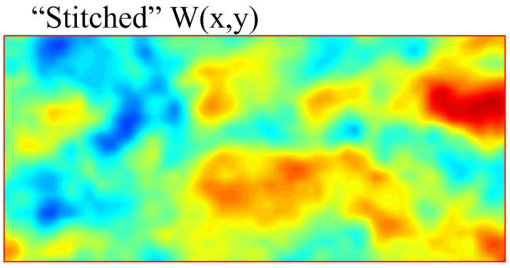

(c) The two frames are averaged in the overlap region forming the "stitched" wavefront

Fig. 3 "Stitching" of two frames $W(x, y, t)$ and $W(x, y, t+\Delta t)$. The flow direction is from left to right.

The algorithm described in Figure [3] is dependant on Taylor's frozen flow hypothesis. We assume that the aero-optical structures do not change in time. This assumption breaks down for a natural shear layer due to the growth of the shear layer. We can begin the process adapting the stitching method to be able to handle the time dependence of shear layer growth by first studying a forced shear layer.

To demonstrate the suppression of shear layer growth over the aperture we can treat the Shack-Hartmann measurements as an array of Malley Probes. The Shack-Hartmann wavefront sensor directly measures deflection angle. We can then plot the deflection angle energy spectra as a function of distance from the splitter plate.

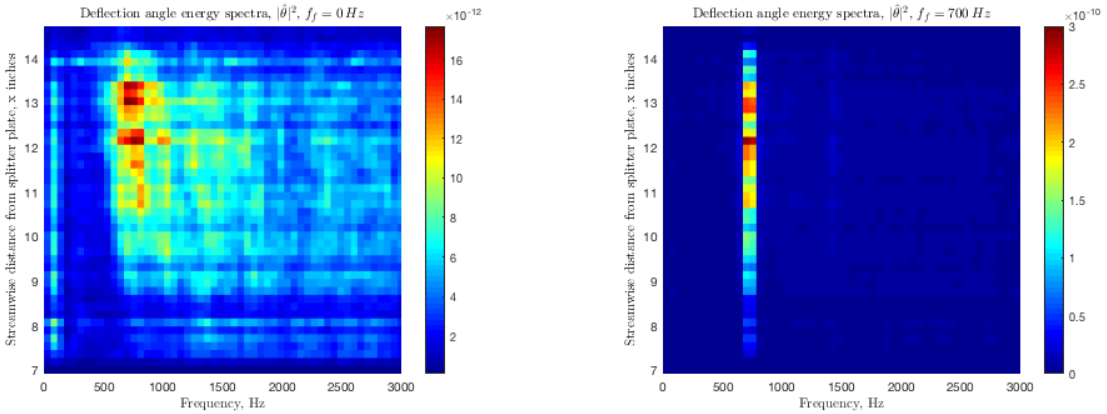

(a) Deflection angle spectra for an unforced shear layer.

(b) Deflection angle spectra for an forced shear layer.

Fig. 4 Deflection angle energy spectra as a function of streamwise position. Forcing regularizes the shear layer over the aperture.

The deflection angle energy spectra for the natural, unforced shear layer can be seen in Figure [4(a)]. The peak in the deflection angle spectra grows in magnitude and shifts toward lower frequencies as you move downstream. This is expected and results from shear layer growth. We can then also plot the deflection angle spectra as a function of streamwise distance for a forced shear layer. This can be seen in Fig. [4(b)].

There is a strong spectral peak at the forcing frequency, f = 700 Hz. Compared to Fig. [4(a)] there is insignificant peak widening as well as a lack of the shift to lower frequencies. This is indicative of a very strong regularized structure passing over the aperture. Using forcing, we have

regularized the shear layer. For the portion over our aperture we have effectively homogeneous flow.

Figure [8], shows an example of a stitched wavefront. The main shear layer structure is periodic and regularized.

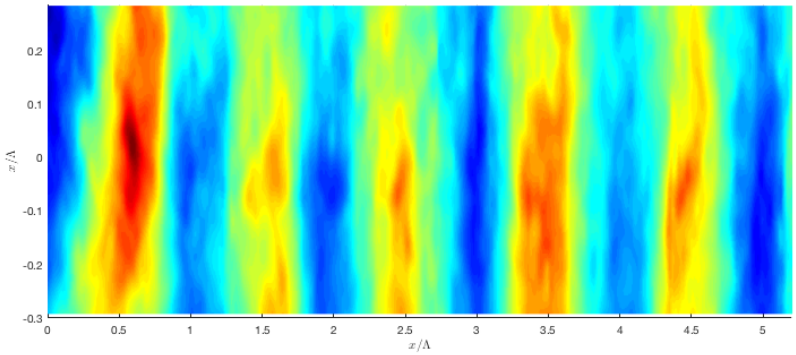

Fig. 5 An example of a stitched wavefront from the shear layer experiment.

A. Modeling

Now that the shear layer has been regularized over the aperture, a model for global jitter can be developed. We can begin by considering the simplest model for the regularized shear layer, a simple sine wave.

1. *Single Sine*

Because the wavefronts are so regular over the aperture due to forcing as seen in Fig. [5] they can be modeled with a simple sine wave. Consider the growing sine wave

$$OPD(x,t) = x\left[sin\left(\left(\frac{2\pi}{\Lambda}\right)(x - U_c t)\right)\right]. \tag{2}$$

Ultimately we are interested in how the jitter changes with aperture. In order to do this, we can consider the spatial OPD^x_{rms}

$$OPD^x_{rms}(Ap,t) = \sqrt{\frac{1}{Ap}\int_0^{Ap}\left[OPD(x,t) - A(t) - xB(t)\right]^2 dx} \tag{3}$$

Here $A(t)$ and $B(t)$ represent the piston and tilt respectively. In other words, for the simple sine wave defined in Eqn. [2] we seek the tilt B(t) as a function of aperture. By definition, the tilt $B(t)$ is simply the value of $B(t)$ that minimizes Eqn. [3]. We can also note that minimizing Eqn. [3]

with respect to A(t) and B(t) is equivalent to minimizing only the integral seen in Eqn. [3]. Thus we have

$$\frac{\partial}{\partial A} = \int_0^{Ap} \left[OPD(x,t) - A(t) - xB(t)\right] dx = 0 \tag{4}$$

$$\frac{\partial}{\partial B} = \int_0^{Ap} \left[OPD(x,t) - A(t) - xB(t)\right] x dx = 0. \tag{5}$$

Eqn. [5] is simply a system of two equations in two unknowns. Rewritten in matrix form we have

$$\begin{bmatrix} \int_0^{Ap} dx & \int_0^{Ap} x\,dx \\ \int_0^{Ap} x\,dx & \int_0^{Ap} x^2\,dx \end{bmatrix} \begin{bmatrix} A(t) \\ B(t) \end{bmatrix} = \begin{bmatrix} \int_0^{Ap} OPD(x,t)\,dx \\ \int_0^{Ap} x \cdot OPD(x,t)\,dx. \end{bmatrix} \tag{6}$$

Solving for $A(t)$ and $B(t)$ we have

$$A(t) = \frac{4AP \int_0^{Ap} OPD(x,t)\,dx - 6\int_0^{Ap} x \cdot OPD(x,t)\,dx}{Ap^2} \tag{7}$$

$$B(t) = \frac{-6\left(Ap \int_0^{Ap} OPD(x,t)\,dx - 2\int_0^{Ap} x \cdot OPD(x,t)\,dx\right)}{Ap^3}. \tag{8}$$

Now that we have an explicit equation for the tilt $B(t)$ we can substitute in the model wavefront from Eqn. [2]. We can then take the rms and we have our single sine model for the forced shear layer. This can be seen in Fig.[6].

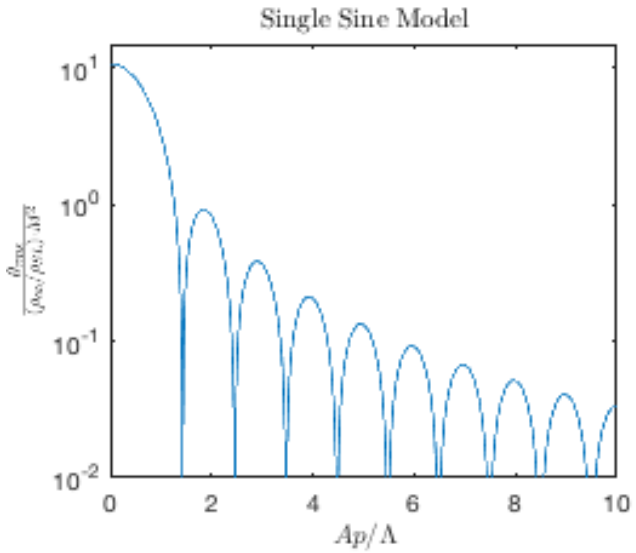

Fig. 6 Normalized rms jitter vs. Ap for the single sine model

2. Filter Model

An obvious improvement to the single sine model would be to include information from more than one frequency in our model. This so-called filter model developed in [7] can be directly applied to the forced shear layer. Once again we begin with a simple harmonic, but this time of arbitrary frequency

$$OPD(x,t) = [sin\left(k_x\left(x - U_c t\right)\right)]\,. \tag{9}$$

By taking the derivative of Eqn. [9] we obtain an equation for the local jitter, $\theta(x,t)$.

$$\theta(x,t) = -k_x cos(\frac{2\pi f}{Uc} \cdot x - 2\pi f t) \tag{10}$$

Continuing along the same logic as with the single sine, we substitute the harmonic wavefront into Eqn. [8] and compute the necessary integrals. This will leave us with a simplified form of the jitter

$$B(t) = -k_x cos(2\pi f t) \cdot G_A(z = Ap/\Lambda) \tag{11}$$

where $G_A(z)$ is

$$G_A(z) = \frac{3[sin(\pi z) - (\pi z) \cdot cos(\pi z)]}{(\pi z)^3} \tag{12}$$

and $z = Ap/\Lambda = (Ap \cdot f)/U_c$. Also, we have $\Lambda = 2\pi/k_x$. We recognize that the first term of Eqn. [11] is simply the phase shifted local jitter. Thus $G_A(z)$ is the global jitter transfer function. A plot of $G_A(z)$ can be seen in Fig. [7].

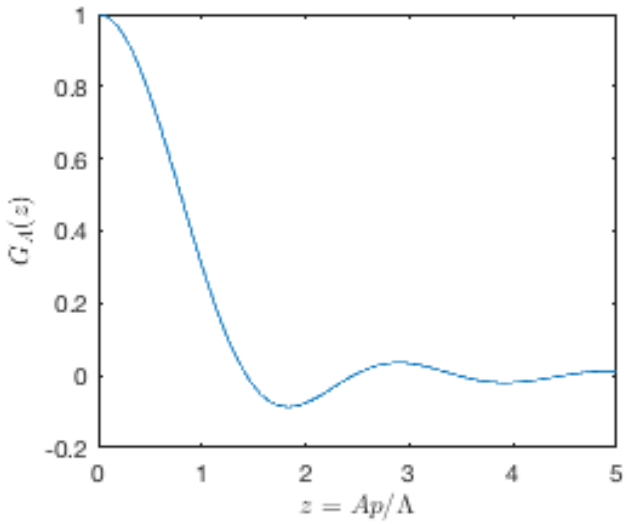

Fig. 7 Global jitter transfer function, $G_A(z)$

$G_A(z)$ transfers the local jitter to the global jitter and overall acts as a kind of low-pass filter. By measuring only the local deflection angle energy spectra, we can determine the global tilt energy spectra. Then by integrating we can compute the global rms jitter for various aperture sizes.

$$\theta_{rms}(Ap) = \int_0^\infty \hat{\theta}(f) \cdot |G_A(z)|^2 \, df \tag{13}$$

B. Variable Aperture Approach

Once the wavefronts have been stitched and corrected for tip/tilt removal we can then begin the process of recovering the aero-optical component of the jitter. The stitching method produces long strips of wavefront data. These strips have been corrected for tip/tilt removal. We can use these long strips of wavefront data and re-aperture them to arbitrary aperture size. We define this re-aperturing process as the Variable Aperture Approach.

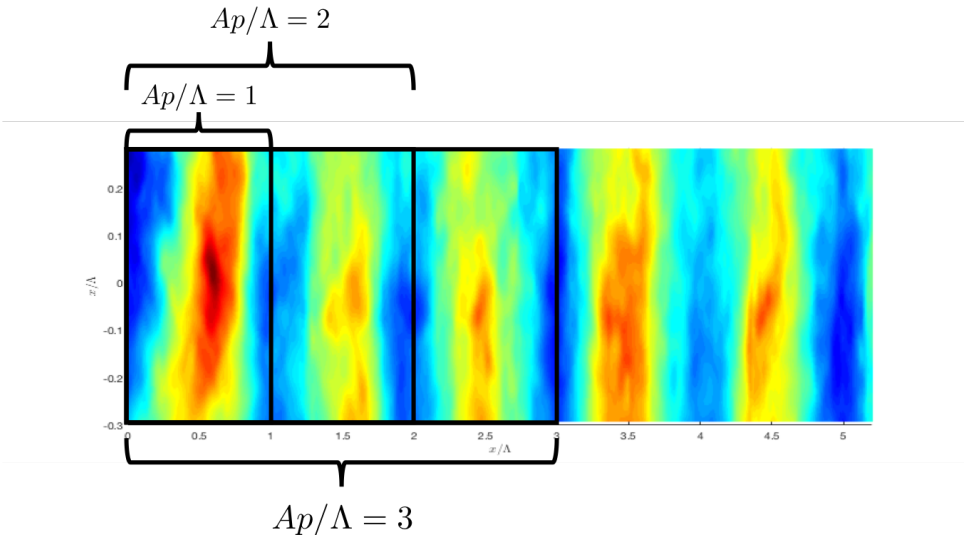

Fig. 8 Variable aperture approach applied to the stitched shear layer data. Λ is defined as the periodic structure size.

It can be seen in Figure [8] that the large wavefront strips generated with the stitching method can be re-apertured arbitrarily. We can then trade space for time and generate time-series of wavefront images. From these new wavefront time series we can then extract the aero-optical component of the jitter.

After the variable aperture approach has been applied, the aero-optical component of the jitter can be extracted. This is done simply by tip/tilt removing the wavefronts and storing the portion of

tip and tilt removed. The tip and tilt left on the wavefronts after applying the stitching method and virtual aperture approach must be from the aero-optics alone. The normalized aero-optical jitter rms for a forced shear layer can be seen in Fig. [III B].

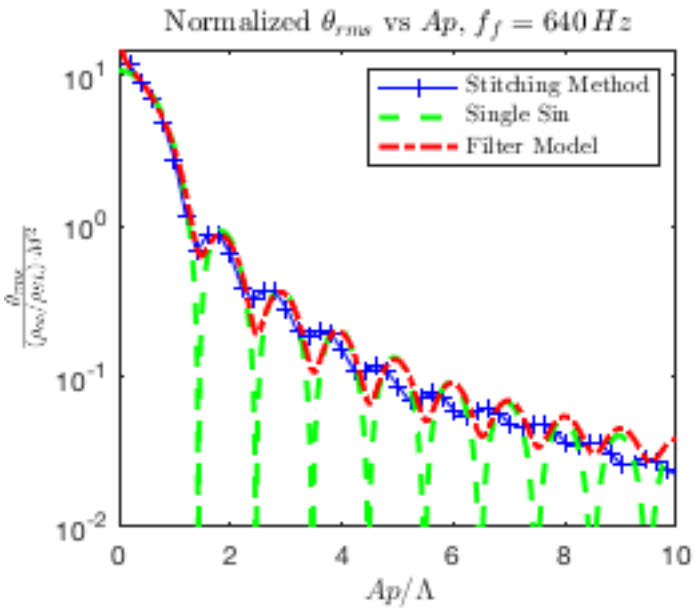

Fig. 9 Normalized jitter rms for the forced shear layer plotted with the analytical prediction

IV. Conclusion

References

[1] Gordeyev, S. and Jumper, E., "Fluid dynamics and aero-optics of turrets," *Progress in Aerospace Sciences*, Vol. 46, No. 8, 2010, pp. 388 – 400, doi:http://dx.doi.org/10.1016/j.paerosci.2010.06.001.

[2] Gladstone, J. H. and Dale, T. P., "Researches on the Refraction, Dispersion, and Sensitiveness of Liquids. [Abstract]," *Proceedings of the Royal Society of London*, Vol. 12, 1862, pp. 448–453.

[3] Siegenthaler, J. P., Gordeyev, S., and Jumper, E., "Shear Layers and Aperture Effects for Aero-Optics," American Institute of Aeronautics and Astronautics, 2005.

[4] Kemnetz, M. R. and Gordeyev, S., "Optical investigation of large-scale boundary-layer structures," in "54th AIAA Aerospace Sciences Meeting," , 2016. AIAA Paper 2016-1460.

[5] Duffin, D. A., "Feed-forward adaptive-optic correction of a weakly-compressible high-subsonic shear layer," , 2009. Copyright - Database copyright ProQuest LLC; ProQuest does not claim copyright in the individual underlying works; Last updated - 2016-03-10.

[6] Ranade, P. M., "Turbulence amplitude modulation in an externally forced, high reynolds number boundary layer," , 2016. Copyright - Database copyright ProQuest LLC; ProQuest does not claim copyright in the individual underlying works; Last updated - 2016-08-17.

[7] Lucca, N. D., Gordeyev, S., and Jumper, E., "The Study of Aero-Optical and Mechanical Jitter for Flat Window Turrets," American Institute of Aeronautics and Astronautics, Aerospace Sciences Meetings, 2012. 05; M1: 0; doi:10.2514/6.2012-623.